

Littman, H., M. H. Morgan III, D. V. Vuković, F. K. Zdanski and Ž. B. Grbavčić, "A Method for Predicting the Relationship between the Spout and Inlet Tube Radii in a Spouted Bed at its Maximum Spoutable Height" in "Fluidization", J. F. Davidson and D. L. Keairns, Eds. Cambridge University Press, Cambridge (1978), pp. 381-386.

Littman, H., M. H. Morgan III, D. V. Vuković, F. K. Zdanski and Ž. B. Grbavčić, "Prediction of the Maximum Spoutable Height and the Average Spout to Inlet Tube Diameter Ratio in Spouted Beds of Spherical Particles", *Can. J. Chem. Eng.* **57**, 684-687 (1979).

Littman, H., M. H. Morgan, III, P. V. Narayanan, S. J. Kim, J. Y. Day and G. M. Lazarek, "An Axisymmetric Model of Flow in the Annulus of a Spouted Bed of Coarse Particles. Model, Experimental Verification and Residence Time Distribution", *Can. J. Chem. Eng.* **63**, 189-194 (1985).

Mamuro, T. and H. Hattori, "Flow Pattern of Fluid in Spouted Beds", *J. Chem. Eng. Japan* **1**, 1-6 (1968).

Mathur, K. B. and P. E. Gishler, "A Technique for Contacting Gases with Coarse Solid Particles", *AIChE J.* **1**, 157-164 (1955).

Mathur, K. B. and N. Epstein, "Spouted Beds", Academic Press, New York (1974).

Morgan, M. H. III and H. Littman, "General Relationships for the Minimum Spouting Pressure Drop Ratio, $\Delta P_{ms}/\Delta P_{mf}$, and the Spout-Annular Interfacial Condition in a Spouted Bed", in "Fluidization", J. R. Grace and J. M. Matsen, Eds., Plenum Press, New York (1980), pp. 287-296.

Mukhlenov, I. P. and A. E. Gorshtein, "Gidravlicheskie soprotivleniye vzveshennogo sloya v bezreshetchnykh konicheskikh apparatakh" (Hydraulic Resistance of Fluidized Beds in Conical Apparatus without a Grate), *Zh. Prikl. Khim.* (Leningrad) **37**, 609-615 (1964).

Mukhlenov, I. P. and A. E. Gorshtein, "Issledovanie fontaniruyushchego sloya" (Investigation of a Spouted Bed), *Khim. Prom-st* (Moscow) **41**, 443-446 (1965).

Nikolaev, A. M. and L. G. Golubev, "Osnovnye gidrodinamicheskie kharakteristiki fontaniruyushchego sloya" (Basic Hydrodynamic Characteristic of a Spouted Bed), *Izv. Vysch. Ucheb. Zaved. Khim. Tekhnol.* **7**, 855-857 (1964).

Povrenović, D. S. "Fluid-Mechanics Characteristics of Conical Spouted Beds", M. S. Thesis, University of Belgrade, Belgrade (1985) (in Serbocroatian).

Romankov, R. G. and N. B. Rashkovskaya, "Sushka vo uzveshennom sostoganii" (Drying in a Suspended State), 2nd Ed., Chem. Publ. House, Leningrad Branch (1968) (in Russian).

Rovero, G., C. M. H. Brereton, N. Epstein, J. R. Grace, L. Casalegno and N. Piccinini, "Gas Flow Distribution in Conical Based Spouted Beds", *Can. J. Chem. Eng.* **61**, 289-296 (1983).

Stanek, V. and J. Szekely, "Three-Dimensional Flow of Fluids Through Nonuniform Packed Beds", *AIChE J.* **20**, 974-980 (1974).

Tsvik, M. Z., M. N. Nabiev, N. V. Rizaev, K. V. Merenkov and V. S. Vyzgo, "Skorosti naruzhenogo fontanirovaniya v sovmeshchenom protsesse polucheniya granulirovannykh udobrenii" (External Flow Rates in Composite Production of Granulated Fertilizers), *Uzb. Khim. Zh.* **11**, 50-51 (1967).

Wan-Fyong, F., P. G. Romankov and N. B. Rashkovskaya, "Issledovanie gidrodinamiki fontaniruyushchego sloya" (Hydrodynamics of Spouted Beds), *Zh. Prikl. Khim.* (Leningrad) **42**, 609-617 (1969).

Manuscript received July 6, 1990; revised manuscript received June 11, 1991; accepted for publication July 8, 1991.

Rotary Cylinders: Transverse Bed Motion Prediction by Rheological Analysis

J. PERRON

École Polytechnique, Montréal, Québec, Canada H3C 3A7

and R. T. BUI*

Université du Québec à Chicoutimi, Chicoutimi, Québec, Canada G7H 2B2

A method for predicting the transverse motion of a granular bed in a rotary cylinder is proposed, based on a non-Newtonian rheological model of the pseudo-plastic type, i.e. with a flow behaviour index (n) between 0 and 1. For a good simulation of bed motion, the model must be able to adequately reproduce the bed velocity profile in both the upper (downward flowing) and the lower (upward moving) zones. It is shown that to do so there is the need to adjust not only the consistency index K but even more importantly the flow behaviour index, n . The mass and momentum conservation equations are solved by the CFD code FLUENT. The model is applied to the simulation of the motion of an alumina bed and the computed results compared with experimental data.

On propose une méthode de prédiction du mouvement transversal d'un lit de particules dans un cylindre rotatif, basée sur un modèle rhéologique non-Newtonien du type pseudo-plastique, i.e. avec indice de comportement n entre 0 et 1. Pour bien représenter ce mouvement, le modèle doit pouvoir reproduire les profils de vitesse dans les deux zones du lit, soit la zone supérieure (où les particules descendent) et la zone inférieure (où elles remontent). On montre que pour ce faire, il faut ajuster non seulement l'indice de consistance K mais aussi et surtout l'indice de comportement n , donc un modèle pseudo-plastique est requis. Les équations de conservation de la masse et du mouvement sont résolues à l'aide du logiciel FLUENT. Le modèle est utilisé pour simuler le mouvement d'un lit d'alumine et les résultats calculés sont comparés avec l'expérience.

Keywords: rotary cylinders, transverse motion, pseudo-plastic rheological model, granular solids.

Horizontal rotary cylinders, slightly tilted on their axes, are commonly used in industrial processes involving particulate materials such as sand, petroleum coke, cement, minerals and agricultural products. The raw material travels along the cylinder axis in a two-component motion: axial transport and transverse movement. While the former is important in determining the residence time of the material within each zone of the cylinder, the latter plays a critical role in ensuring bed homogeneity and uniform treatment of the bed material as determined by its exposure to the free-board gas. In a previous work (Perron and Bui, 1990), a model for the prediction of axial transport in a rotary cylinder was proposed. The purpose of this work is to study the isothermal transverse motion of a bed of particulate materials.

Transverse motions vary widely from one situation to the next. The type of movement can be determined from the speed of rotation of the cylinder and the properties of the bed material. Usually, with increasing rotation speed, the modes observed are successively: slipping, rolling, cascading, cataracting, and centrifuging. Transition between modes can be determined by calculating the relevant characteristic parameters (Rutgers, 1965; Henein et al., 1983).

Several previous authors have studied the axial transport in rotating cylinders: Sullivan (1927), Bayard (1945), Friedman (1949), Saeman (1951), Vahl (1952), Kramers (1952), Ronco (1960), Perry (1961), Zablony (1964), Heiligenstaedt (1971) and Perron and Bui (1990). All these studies proposed correlations to predict the mean axial velocity and therefore the residence time. The investigators usually started with experiment-based assumptions and the fundamentals of physics such as mass conservation, and derived an expression for the axial transport velocity. Surveys of such work can be found in Zablony (1964) and Perron and Bui (1990).

*Correspondence to R. T. Bui.

Transverse motion studies are more recent. A review of the literature reveals a clear trend in the evolution of models used to represent transverse motions in kilns. Early investigators assumed an infinitely thin layer at the bed surface, in which the material moved downward with the rest of the bed forming a lower zone in which the material went upward in a plug flow movement (Figure 1a). This was the case with Saeman (1951), Vahl and Kingma (1952), Kramers (1952), Carley-Macaulay and Donald (1962) and Zablony (1964). Later came the assumption of an upper zone of finite thickness, where the material moved downward, while in the lower zone the motion was upward in plug-flow (Figure 1b). This was the case with Rutgers (1965) and Mu and Perlmutter (1980). More recently, the upper zone was taken to be in a crescent shape with an internal velocity profile, while the lower zone, also crescent shaped, experienced plug-flow movement (Figure 1c). The work of Lehmborg et al. (1975), Tscheng (1978), Henein et al. (1983), Barr (1986) and Perron and Bui (1990) belong to this category.

In this work, the isothermal transverse motion of an alumina particle bed will be studied using the laws of continuum mechanics to model the rheological behaviour of the bed material.

The problem and the simplifying assumptions

Let a cylinder at rest and partially filled with a granular material be suddenly submitted to a rotation at constant angular velocity. At first, the material climbs up the cylinder wall in a bulk motion until a critical value of the dynamic friction angle is reached. Then the particles located at the top part of the bed start rolling down along the bed surface. After a short time, steady state is reached providing that the speed of rotation of the cylinder remains constant. Every time this speed changes, a small change in the dynamic friction

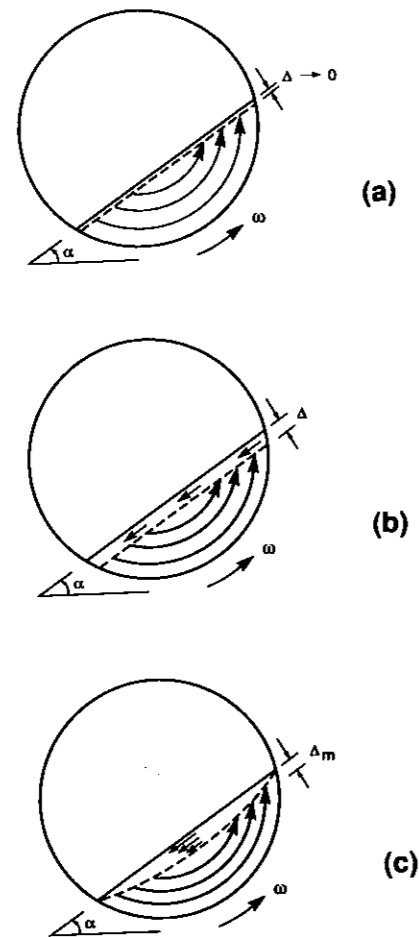


Figure 1 — Assumptions made to represent transverse motion in rotating cylinders: (a) thin cascading layer; (b) finite thickness cascading layer; (c) crescent shape cascading layer.

angle is observed. If the speed increases appreciably, the bed surface takes on a slightly wavy form with a crest near the top of the bed and a trough near the lower end.

Clearly, the position and shape of the bed surface are determined by the forces involved, namely the forces of friction, of inertia, and of gravity, each with a normal and a tangential component. Thus, for a high rotation speed, the particles at the top end of the bed can be ejected upward out of the bed, resulting in a local deformation of the bed surface. Knowledge of these forces acting on the particles helps determine the motion of the particles and therefore the bed shape. Essentially the problem is that of a body of particles submitted to an ensemble of forces, the latter being influenced by the form and density of the particles, and the rotational speed and inner surface roughness of the cylinder.

A formal analogy exists between the elastic and viscous fluid mechanical problems (Zienkiewicz, 1977). The displacement, strain, stress and shear modulus in elasticity find their viscous fluid analogies in the velocity, strain rate, stress and viscosity, respectively. The granular bed can be treated as an incompressible viscous fluid, to which the known analysis techniques for incompressible elasticity are readily applicable. The bed can also be seen as a continuum, as particle size is small compared to bed dimensions.

The following simplifying assumptions apply:

- only the rolling mode of particle motion is considered. This is a reasonable assumption considering the range of rotational speed, e.g. 2 to 5 rpm commonly encountered in industrial kilns.

- particle motion, particle average velocity profiles and bed shape are in steady state.
- bed surface transverse profile is a straight line.
- particle flow as a whole is laminar.

Methodology

The mass and momentum conservation equations (Navier-Stokes equations) applied to the body of particles are solved using FLUENT, a fluid dynamic software with finite-volume discretization and finite-difference formulation, based on the SIMPLE algorithm. For a review of Navier-Stokes equations, an appropriate reference is Ryhming, (1985). The successive steps in the methodology applied in this work are as follows:

- 1- select among the existing rheological models those that are applicable to granular materials.
- 2- apply these rheological models to the experimental data reported by Tscheng (1978) for a bed of alumina particles.
- 3- choose a discretization scheme suitable to the geometry of the problem at hand.
- 4- solve the equations of conservation using FLUENT.
- 5- compare the computed bed velocity profiles obtained with each rheological model with Tscheng's (1978) data.
- 6- identify a rheological model that best fits the problem.

The rheological models

The general stress-strain rate relationship may take various forms, a typical one being given by the Ostwald power law:

$$\bar{\sigma} = K \dot{\epsilon}^n = (K \dot{\epsilon}^{n-1}) \dot{\epsilon} \quad \dots \quad (1)$$

where

$$\eta = K \dot{\epsilon}^{n-1} \quad \text{and} \quad \bar{\sigma} = J_2^{0.5} \quad \dots \quad (2)$$

The second invariant J_2 of the stress deviator tensor S_{ij} is:

$$J_2 = \frac{1}{2} S_{ij} S_{ij}$$

For a Newtonian fluid, the viscosity η is equal to K , and the flow behaviour index is $n = 1$. For a pseudo-plastic fluid, $n < 1$, and $n > 1$ for a dilatant fluid. The rheological behaviour of the granular material must be determined in order to obtain an expression for η to be introduced in the Navier-Stokes equations. Various models exist for η as applied to granular materials with inter-particle void. Presented below are four such models obtained by past workers through different approaches.

Model 1.

Starting with a dimensional and rheological analysis of the motion of a granular material in a rotating cylinder, Perron and Bui (1990) derived an expression for the bed apparent viscosity:

$$\eta = (\rho g / R \Gamma \omega) [h^2 \cos \alpha + 2h(2hR - h^2)^{0.5} \sin \alpha] (1 - \cos 0.5\Gamma) (1 + 2 \tan 0.5\Gamma/\Gamma)^{-1} \quad \dots \quad (4)$$

The above relation is valid for an isothermal, steady-state system, in which the bed motion is in a rolling mode. Perron and Bui (1990) did not address the problem of predicting a numerical value for the flow behaviour index n . However, clearly an initial stress is required to start the particle motion; therefore, n must be < 1 in order to approximate the ideal behaviour of a Bingham fluid (Miller, 1983).

Model 2

Using the experimental data coming from a study of the transport properties of gas-particles mixtures, Schugel (1971) derived an empirical correlation for the apparent viscosity, assuming that the interactions between particles are non-Newtonian in nature. He obtained:

$$\eta = (4/2.65 \times 10^{-2}) (4.61/4) r^2 \rho_p \phi^2 / (\phi_o - \phi)^2 \quad (5)$$

where ϕ is the solid volume fraction of the granular material, and ϕ_o is the maximum value of ϕ taken as 0.6. Schugel's (1971) model is valid for the interval:

$$2 < \phi / (\phi_o - \phi) < 25$$

Model 3

Some years later, to account for the inter-particle collisions with better accuracy, Sha and Soo (1977) suggested an empirical correlation based on Schugel's (1971) work. The expression for apparent viscosity then became:

$$\eta = (4/2.65 \times 10^{-2}) r^2 \rho_p \{ [a_2 \phi^2 / (\phi_o - \phi)^2] + [a_3 \phi^3 / (\phi_o - \phi)^3] + [a_4 \phi^4 / (\phi_o - \phi)^4] \} \quad (6)$$

where $a_2 = 1.650$
 $a_3 = -0.2709$
 $a_4 = 0.01114$

The expression was obtained for an expanding bed of solid volume fraction $\phi = 0.52$. The work of Sha and Soo (1977) is valid for the interval:

$$2 < \phi / (\phi_o - \phi) < 14$$

In Schugel's (1971) as well as the work of Sha and Soo (1977) no additional information on the possible values for n was given.

Model 4

In elasto-plasticity, it is generally admitted that beyond the elastic limit of the material, plastic flow takes place. Plastic flow starts when the stress reaches an upper limit. For an isotropic material, the flow rule has the general form:

$$F = f(\sigma_{ij}) - g(k) = 0 \quad \dots \quad (7)$$

where f is a function of stresses σ_{ij} , g an experimentally determined parameter of the material, and k a strain hardening parameter.

For frictional materials such as concrete, soil, petroleum coke, the Mohr-Coulomb flow rule and an approximation of it known as Drucker-Prager model, are frequently used (Brebba et al., 1984):

$$\alpha' I_1 + \bar{\sigma} - K' = 0 \quad \dots \quad (8)$$

$$\alpha' = \tan \beta (9 + 12 \tan^2 \beta)^{-0.5} \quad \dots \quad (9)$$

$$K' = 3C (9 + 12 \tan^2 \beta)^{-0.5} \quad \dots \quad (10)$$

where C is the cohesion factor, and β the internal friction angle of the material. For an isotropic fluid, the mean stress σ_m is given by:

$$\sigma_m = I_1 / 3 = -P \quad \dots \quad (11)$$

where P is the pressure and I_1 the first invariant of the stress tensor σ_{ij} :

$$I_1 = \sigma_{11} + \sigma_{22} + \sigma_{33} \quad \dots \quad (12)$$

Substituting the general stress-strain rate relation, Equation (1), into the Drucker-Prager model, Equations (8), (9) and (10), and solving for η , one obtains the following expression for the apparent viscosity:

$$\eta = 3 (9 + 12 \tan^2 \beta)^{-0.5} (C - 0.333 \tan \beta) / \dot{\epsilon} \quad (13)$$

or, by substituting Equation (11) into Equation (13):

$$\eta = 3 (9 + 12 \tan^2 \beta)^{-0.5} (C + P \tan \beta) / \dot{\epsilon} \quad \dots \quad (14)$$

Application to experimental data

Tscheng (1978) studied the transverse motion of alumina particles by tracing them using photographic means. He thus obtained their trajectories and velocities at various positions in the bed. The experimental conditions used were as follows:

internal radius of cylinder	$R = 0.0975$ m
average radius of alumina particles	$r = 0.0031$ m
speed of rotation of cylinder	$\omega = 0.500$ rad/s

From the above specified experimental conditions and from the photographic records of the bed, the following data can be derived:

height of bed	$h = 0.066$ m
dynamic friction angle	$\alpha = 0.7$ rad
filling angle	$\Gamma = 2.48$ rad
maximum bed width	$S = 0.187$ m

The other data needed are taken as follows:

density of alumina particles	$\rho_p = 3630$ kg/m ³
solid volume fraction of bed material	$\phi = 0.523$
bulk density of bed material	$\rho = 1900$ kg/m ³

This value of ϕ is obtained by assuming that the spherical-shaped alumina particles are stacked squarely in lattices, thus giving $\phi = (4/3) \pi^3 / 8r^3 = 0.523$. The bulk density is taken as the particle density multiplied by the solid volume fraction ϕ .

With these data, the apparent viscosity of the bed can now be evaluated using three of the four models listed previously. These are models numbered 1 to 3. As for model 4, one more

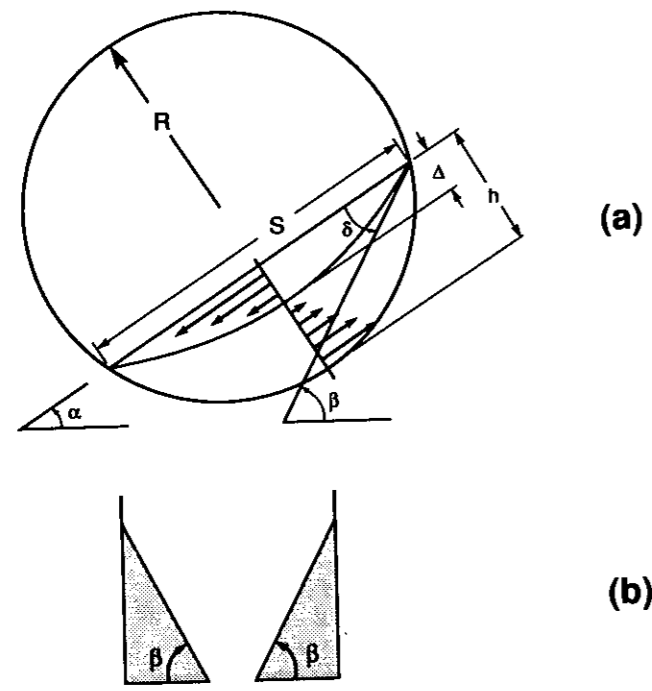


Figure 2 — Geometry of transverse section of bed. (a) definition of dynamic friction angle α and internal friction angle β . (b) analogy with internal friction angle defined by Kunii.

parameter needs to be determined, namely the internal friction angle of the granular material.

The values of η thus obtained with models 1, 2 and 3 are 374, 299 and 95 kg/m · s, respectively.

By analogy with the internal friction angle for a flow of particles through an opening at the center of the bottom of a vertical cylinder (Kunii and Levenspiel, 1962), the internal friction angle for the granular materials in a rotating cylinder may be defined as angle β in Figure 2. It is the angle formed by the horizontal line with the tangent to the interface between the upper and the lower sub-crescents. The analogy is justified by the fact that in both cases, angle β cannot grow larger without causing a downpour of particles from the top of the pile along its slope.

From Figure 2 we have

$$\beta = \alpha + \delta \quad (15)$$

From a simple relation of geometry applied to the arc lengths of a circle, we have:

$$\delta = 2 \tan^{-1} (\Delta / 0.5 S) \quad (16)$$

where Δ is the maximum depth of the upper sub-crescent, and $0.5 S$ is the half-width of the bed surface. From the experimental data of Tscheng (1978), angle β can be readily evaluated to be 59° or 1.03 rad.

By analogy with the work of Maeda and Matsunaga (1989), in which a granular flow through a rectangular duct was studied using the Drucker-Prager model with a cohesion factor $C = 0$, in this case C is also taken to be 0.

The pressure P in Equation (11) results from the force of gravity prevailing at the given location:

$$P = \rho g \ell \quad (17)$$

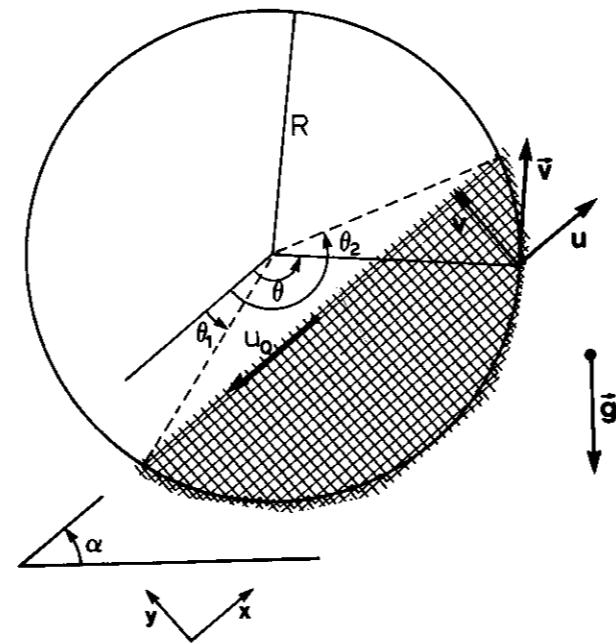


Figure 3 — Domain discretization and definition of coordinates. The reference from which θ is measured is the direction of the bed surface, given by α .

where ℓ is the height of the point considered inside the bed, measured vertically. A bulk approximation for the mean value of ℓ , denoted by $\bar{\ell}$, is:

$$\bar{\ell} \cong 0.5 S \sin \alpha \quad (18)$$

which, applied to Tscheng's (1978) case, yields $\bar{\ell} = 0.060$ m.

Substitution of the above numerical values into Equation (14) yields the following expression for the apparent viscosity of the bed:

$$\eta \cong 863 / \dot{\epsilon} \quad (19)$$

A comparison of Equations (19) and (2) leads to the conclusion that the flow of alumina particles in the bed can be approximated by a non-Newtonian flow with a consistency index $K = 863$ kg/m · s²⁻ⁿ and a flow behaviour index $n = 0$. Therefore, under the assumption that the Drucker-Prager model applies, Tscheng's (1978) alumina bed can be considered to behave in ideal plastic flow, i.e. with a constant stress independent of the strain rate.

Computational aspects

The domain considered is the two-dimensional cross-section of the granular bed. The x - and y -directions are defined as in Figure 3. Gravity g is considered in the x - and y -directions and neglected in the axial direction of the cylinder due to the small tilt, usually 2 to 3°.

Discretization is done in cartesian coordinates along x and y . Polar coordinates would be inconvenient since the actual percent fill of the cylinder is usually less than 0.5. Body-fitted coordinates yield a better match with the domain's geometry, but cause convergence difficulties at the cells near the corners. These cells suffer from a serious lack of orthogonality, required to facilitate convergence.

TABLE I
Rheological Models Used in the Simulations

Type of model	Name of Model	$K =$ [kg/m · s ²⁻ⁿ]	$n =$	Simulation Case No.	See Figures	
Newtonian ($n = 1$; $\eta = K$)	Perron-Bui (1990)	374	1	1	4 and 5	
	Schugel (1971)	299	1	2		
	Sha and Soo (1977)	95	1	3		
non-Newtonian	pseudo plastic ($n < 1$)	Perron-Bui (1990)	374	0.75	4	6 and 7
			374	0.50	5	
			374	0.05	6	
	ideal plastic ($n = 0$)	Drucker-Prager (Brebba et al., 1984)	863	0.05	7	

Note: In case #7, n is taken as 0.05 instead of 0 simply to accelerate convergence.

The grid is composed of 648 cells. Such a refinement is appropriate for a good visualization of the velocity profiles in different parts of the bed. The boundary conditions are given below. At the cylinder wall:

$$u = R\omega \sin \theta \quad (20)$$

$$v = -R\omega \cos \theta \quad (21)$$

$$\theta_1 \leq \theta \leq \theta_2 \quad (22)$$

where θ_1 and θ_2 are defined by bed position as indicated on Figure 3.

At the bed surface:

$$u = u_0 \quad (23)$$

$$v = 0 \quad (24)$$

Care must be taken to avoid the false numerical diffusion stemming from the non-alignment of the cartesian grid with the tangential velocities along the rotary vessel's wall. One way of assessing false diffusion is to compute an expression suggested by Patankar (1980) based on the work of De Vahl Davis and Mallinson (1972) for a two-dimensional cartesian grid:

$$D_f = \rho v \Delta x \Delta y \sin 2\gamma / 4 (\Delta y \sin^3 \gamma + \Delta x \cos^3 \gamma) \quad (25)$$

where: v is the velocity at the point considered, Δx and Δy are the cell's dimensions (0.00368 m; 0.00382 m) and γ is the angle made by the velocity vector v with the x -direction (0 to 90°).

De Vahl Davis and Mallinson (1972) proposed to take $\gamma = 45^\circ$, which would yield a maximum value for D_f in order to be on the safe side. Then

$$D_f = 0.12 \text{ kg/m} \cdot \text{s} \quad (26)$$

This value is small compared to the order of magnitude of η coming from any of the four rheological models. It can be said, therefore, that in this problem false diffusion generation is negligible.

Next, a check is carried out to ensure that the thickness of the boundary layer is greater than the half-length of a cell, so that the near-wall velocity profile be correctly represented.

The boundary layer thickness can be approximated with that for a plane surface in laminar flow:

$$\nu \cong 5 \bar{x} / Re^{0.5} \quad (27)$$

where \bar{x} is the longitudinal position of the point considered, in the flow direction.

In this problem, we consider the mid-point of the circular arc covered by the granular bed. Therefore, the distance \bar{x} is the half-length of that arc:

$$\bar{x} = R (\Gamma / 2) = (0.0975) (2.48 / 2) = 0.12 \text{ m} \dots (28)$$

and Re is taken as

$$Re = u_\infty S \rho / \eta \cong 0.9 \quad (29)$$

Then we have

$$\nu = 5 \times 0.12 / 0.90^{0.5} = 0.63 \text{ m} \quad (30)$$

This boundary layer thickness is several orders of magnitude greater than the cell dimensions. Therefore the condition for the representation of the velocity profile at the cylinder wall is generously satisfied.

The conservation equations are solved for mass and momentum using FLUENT. The under-relaxation factors used for pressure and velocities u and v are 0.5, 0.2 and 0.2, respectively. Convergence taken to be reached when the sum of the residues for p , u and v is less than 10^{-3} .

Analysis of results

Table 1 shows the results of the seven simulations that have been carried out, with the corresponding rheological methods used, of which three are Newtonian ($n = 1$) and four are non-Newtonian. Among the latter, three are pseudo-plastic ($n < 1$) and one is ideal plastic ($n = 0$). Note in Table 1 that for the ideal plastic case, n is taken as 0.05 instead of 0 simply to accelerate numerical convergence.

To avoid overcrowding the figures, the simulations are classified into two groups, namely the ones with Newtonian models (cases 1 to 3) and the ones with non-Newtonian models (cases 4 to 7). Such a classification is natural and appears to be even more so when comparison is made between the respective velocity profiles obtained by cutting

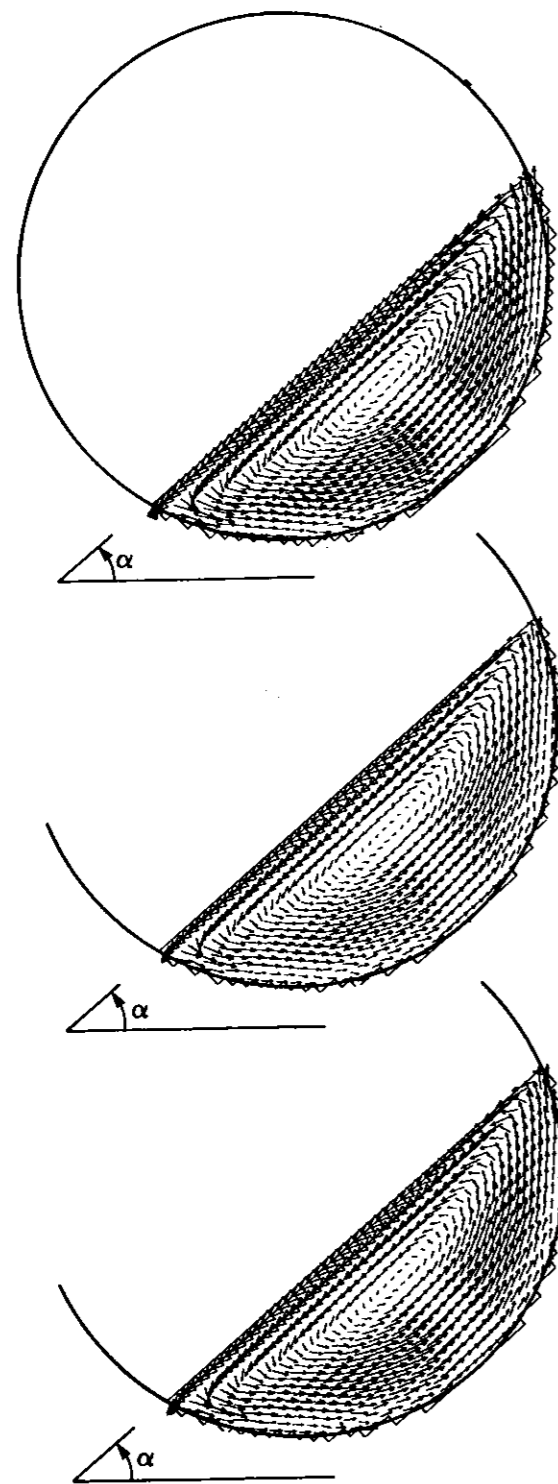


Figure 4 — Velocity fields obtained with three Newtonian models. #1: Perron-Bui (1990), #2: Schugel (1971), #3: Sha and Soo (1977).

radially through the mid-point of the bed. For the Newtonian models, Figure 5 shows a sharply curved velocity profile inside the lower, upward-moving sub-crescent. For the non-Newtonian models, Figure 7 shows that this velocity profile displays a much flatter form. A detailed analysis of the results is given below.

RESULTS OF SIMULATIONS USING THE NEWTONIAN-TYPE RHEOLOGICAL MODELS

Results of simulation cases 1 to 3 are presented in Figures 4 and 5. Figure 4 shows the velocity fields obtained with the

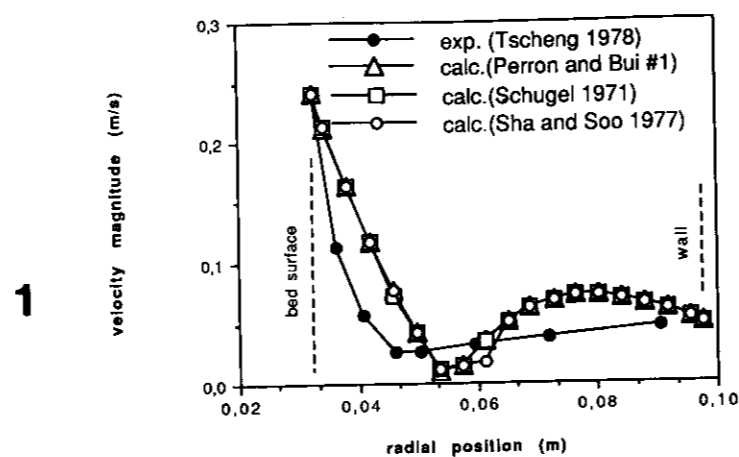


Figure 5 — Velocity profiles in cross-section of bed, for the three Newtonian models.

three Newtonian models corresponding to three different values of viscosity namely 374, 299 and 95 kg/m · s. The three velocity fields are similar and do not change significantly with the change in the viscosities. In all three cases, a central recirculation zone exists. The velocity vectors display a regular behaviour especially near the wall, and numerical convergence is readily reached. The upper, downward-flowing sub-crescent has a depth of 0.021 m at its center for all three cases. Note that Tscheng's (1978) experimental value of the upper layer is 0.015 m. Thus, the Newtonian models over-estimate the depth of this active layer by some 40 percent.

Figure 5 shows the profiles of the velocity magnitudes in a cross-section at the mid-point of the bed. The curves give the velocity variations for different radial positions. Tscheng's (1978) experimental data are also included for comparison. The three calculated velocity profiles coming from the three cases are very similar. From the bed surface, the velocities decrease rapidly as the bed depth increases, but not rapidly enough to match the data of Tscheng (1978). The profiles also show that the calculated upper sub-crescent thickness is over-estimated compared to the experimental value. In the lower sub-crescent, the calculated velocity profiles are significantly different from the experimental one: the former are curved with convexity pointed in the flow direction, while the latter is flat, meaning that the bulk motion observed experimentally is close to plug flow.

Thus, the Newtonian models succeed in predicting the overall shape of the velocity field and of the velocity profile, but serious discrepancies exist when velocities are determined at a given bed depth. Also, the plug-flow motion inside the lower sub-crescent cannot be adequately reproduced by Newtonian models.

RESULTS OF SIMULATIONS USING THE NON-NEWTONIAN-TYPE RHEOLOGICAL MODELS:

Results of simulation cases 4 to 6 are presented in Figures 6 and 7. These correspond to the pseudo-plastic rheological models, with flow behaviour index $n < 1$. As shown in Table 1, as the starting point a consistency index of $K = 374 \text{ kg/m} \cdot \text{s}^{2-n}$ is used, which comes from the K value determined with the Perron-Bui (1990) Newtonian-type model (case 1). But here, various values for n are tried in an endeavour to best match Tscheng's (1978) experimental data. Thus n is given the values of 0.75, 0.5 and 0.25 successively.

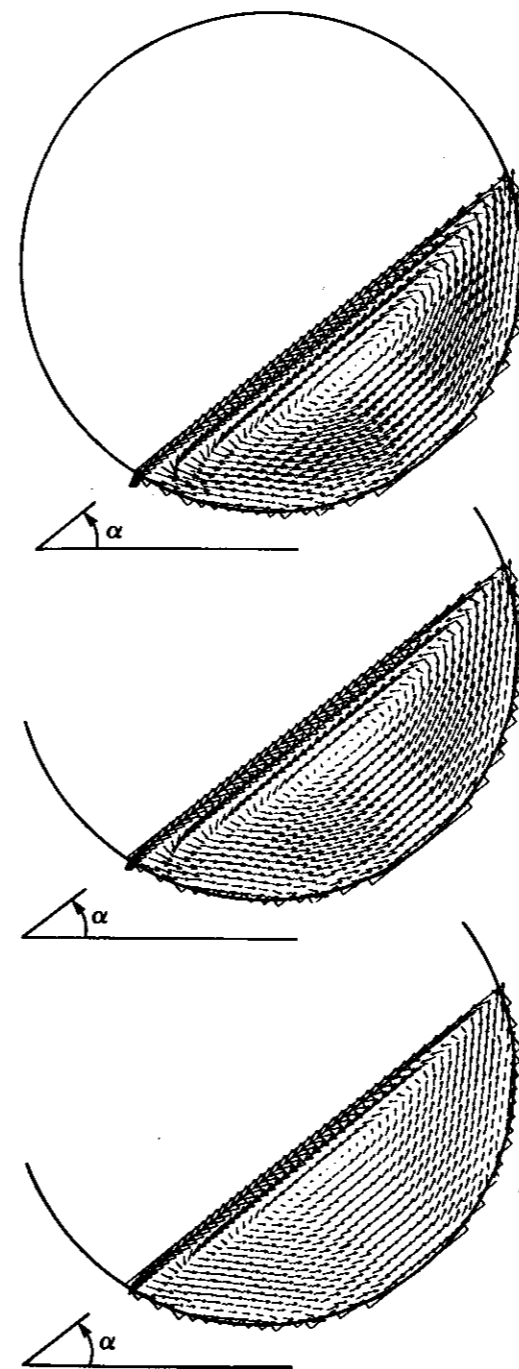


Figure 6 — Velocity fields obtained with non-Newtonian, pseudo-plastic models, $K = 374 \text{ kg/m} \cdot \text{s}^{2-n}$; #4: $n = 0.75$, #5: $n = 0.5$, #6: $n = 0.25$.

Figure 6 presents the calculated velocity fields for each of the three cases. The depth of the upper sub-crescent decreases as n decreases. It is 0.021, 0.017 and 0.0134 m for $n = 0.75, 0.5$ and 0.25 , respectively. As Tscheng's (1978) experimentally determined depth is 0.015 m, the value of $n = 0.5$ suits best. Numerical convergence was obtained for cases 4 and 5 after 1339 and 1500 iterations, respectively, which is roughly twice the number of iterations required for the Newtonian models. Case 6 did not converge after 2000 iterations, but the sum of residues then stabilized at 2.6×10^{-2} .

It can be seen in Figure 6 that at the right end of the bed surface, the velocity vectors display a general direction orthogonal to the bed surface and pointing outward, while

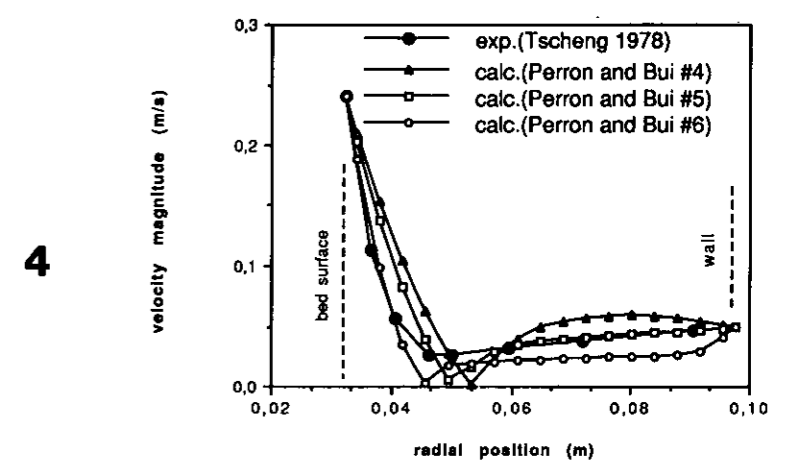


Figure 7 — Velocity profiles in cross-section of bed, for the three pseudo-plastic models.

the opposite occurs at the left end of the bed surface, i.e. velocity vectors orthogonal and pointing inward. This may be the phenomenon that contributes to the slightly wavy form of the bed surface, with a crest at the right end and a trough at the left end, as previously mentioned.

Figure 7 shows the profiles of velocity magnitude in a cross-section at mid-point of the bed. Compared to the Newtonian models of cases 1 to 3, these pseudo-plastic models do a better job in reproducing the velocity profiles in the upper sub-crescent. The various numerical values assigned to the flow behaviour index n allow an adjustment of that part of the velocity profile to match the experimental data. This adjustment was not possible with the Newtonian models. From Figure 7, it is noted that the smaller the value of n , the thinner the upper sub-crescent, and the flatter the velocity profile in the lower sub-crescent. Also, for small values of n , the flow behaviour approaches that of an ideal fluid (zero viscosity), thus reducing the viscous entrainment effect by the wall on the adjacent bed layers, and therefore lowering the average bed velocity.

In summary, it appears that the use of a pseudo-plastic model is the best way to describe the rheological behaviour of the granular bed. Adjusting the value of n between 0 and 1 allows us to match the experimental velocity profile in both upper and lower sub-crescents. For alumina, Figure 7 shows that case 5 with $n = 0.5$ yields the nearest match.

RESULTS OF SIMULATION USING THE IDEAL PLASTIC RHEOLOGICAL MODEL

Results of simulation case 8 are presented in Figures 8 and 9. The flow here is the ideal plastic flow resulting from the application of the Drucker-Prager model (Equations 8, 9 and 10) that yields $K = 863 \text{ kg/m} \cdot \text{s}^2$ and $n = 0$. The computation fails to converge even after 4000 iterations, but the residues stabilize at 3.4×10^{-2} . The more remote a model is from the Newtonian model, the more difficult it is to obtain convergence, and the higher the number of iterations required. In this case, instead of $n = 0$, a value of $n = 0.05$ has been assumed in order to obtain convergence.

Figure 8 shows that the average bed velocity has decreased considerably. The upper sub-crescent becomes very thin. The lower sub-crescent is accordingly enlarged, but particle movement there is slow. In fact, Figure 9 shows a velocity profile that is so low that clearly it cannot match the experimental profile.

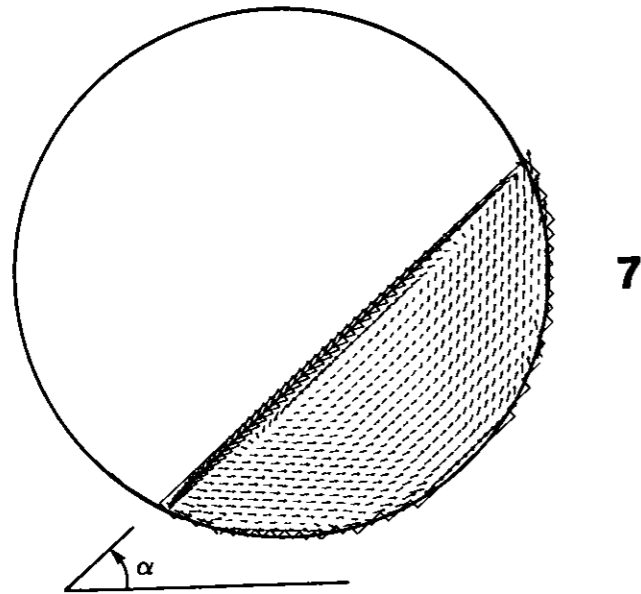


Figure 8 — Velocity field obtained with ideal plastic Drucker-Prager model (Brebba et al., 1984).

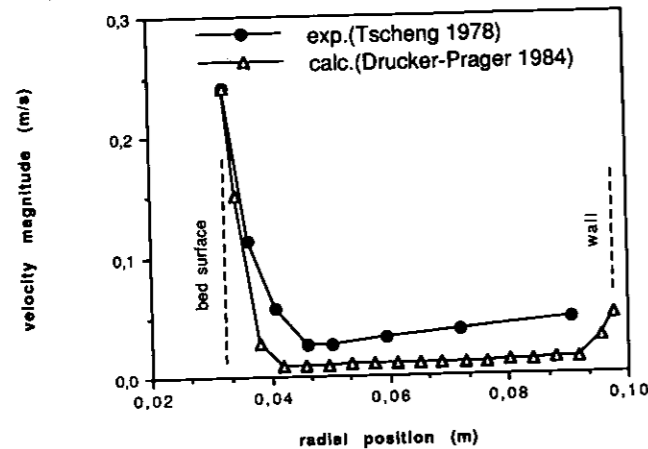


Figure 9 — Velocity profile in cross-section of bed for the ideal plastic Drucker-Prager model (Brebba et al., 1984).

Conclusions

It has been shown that the transverse motion of a granular bed in a rotating cylinder can be adequately approximated as a pseudo-plastic fluid flow using the laws of fluid dynamics. In this work, no particular attention was paid to the effects of particle size or cylinder diameter, the assumption being that the former must be small enough compared to the latter so that the bed can be treated as a continuum. It was found that neither a Newtonian model ($n = 1$) nor an ideal plastic model ($n = 0$) could satisfactorily reproduce the two-zone transverse motion of the bed, while a non-Newtonian model, of the pseudo-plastic type ($0 < n < 1$) is by far more suitable. For a good representativity, the velocity profile, especially that of the lower zone next to the cylinder wall, must be adequately reproduced. As this velocity profile varies considerably with the intensity of the viscous entrainment of the wall on the successive layers of the bed material, it is critically important that a tuning can be made by varying the flow behaviour index, and therein lies the great advantage of a pseudo-plastic model.

The often reported sub-crescent shape of the two zones was clearly predicted. Tscheng's (1978) experimental

velocity profile in both zones was well reproduced. For alumina, the flow behaviour index was estimated to be $n = 0.5$ for a consistency index of $K = 374 \text{ kg/m} \cdot \text{s}^{2-n}$.

For values of n near zero, numerical convergence was difficult to obtain. The number of iterations required to reach a stable residue was found to be approximately inversely proportional to $n^{3/2}$. Use of a cartesian grid gave a realistic visualization of the flow pattern inside the bed and at the bed surface, especially its two ends.

In this work, the transverse profile of the bed surface was assumed to be a straight line. Carrying on further, the pseudo-plastic model can be coupled with an algorithm to calculate the form of the free surface of the bed. Then it will be possible to completely determine the bed shape and motion for various rotational speeds of the cylinder. This appears to be an avenue for further investigation susceptible of giving a complete integrated model of a granular bed in a rotary cylinder.

Nomenclature

- a_2 = coefficient, —
- a_3 = coefficient, —
- a_4 = coefficient, —
- C = cohesion factor [N/m^2]
- D_f = false numerical diffusion [$\text{kg/m} \cdot \text{s}$]
- f = function of stresses [N/m^2]
- F = flow rule [N/m^2]
- g = parameter of material [N/m^2]
- h = bed depth [m]
- l = bed height measured vertically [m]
- I_1 = first invariant of stress tensor [N/m^2]
- I_2 = second invariant of the deviatoric stress tensor [N^2/m^4]
- k = strain hardening parameter, —
- K = consistency index [$\text{kg/m} \cdot \text{s}^{2-n}$]
- K' = Drucker-Prager model constant [N/m^2]
- n = flow behaviour index, —
- P = pressure [N/m^2]
- r = radius of particles [m]
- R = radius of cylinder [m]
- Re = Reynolds number = $u_o \rho / \eta$, —
- S = bed width [m]
- S_{ij} = stress deviator tensor [N/m^2]
- u = x -velocity [m/s]
- u_o = x -velocity at bed surface [m/s]
- v = y -velocity [m/s]
- x = coordinate, —
- \bar{x} = half-length of arc covered by bed [m]
- y = coordinate, —
- Δx = dimension of cell [m]
- Δy = dimension of cell [m]

Greek letters

- σ_{ij} = stress tensor [N/m^2]
- $\bar{\sigma}$ = stress [N/m^2]
- σ_m = mean stress [N/m^2]
- α = dynamic friction angle [rad]
- α' = Drucker-Prager model's constant, —
- ρ = bulk density [kg/m^3]
- ρ_p = density of particle [kg/m^3]
- ϕ = solid volume fraction, —
- ϕ_o = maximum solid volume fraction, —
- δ = angle included in upper sub-crescent of bed [rad]
- Δ = depth of upper sub-crescent [m]
- γ = angle of velocity vector v with x -direction [rad]
- θ = angle [rad]
- ν = thickness of boundary layer [m]

- β = internal friction angle [rad]
- ω = speed of rotation [rad/s]
- Γ = filling angle [rad]
- μ = dynamic viscosity [$\text{kg/m} \cdot \text{s}$]
- η = apparent viscosity [$\text{kg/m} \cdot \text{s}$]
- $\dot{\epsilon}$ = strain rate [s^{-1}]

Subscripts

- p = particles
- i, j = tensor notation

References

- Barr, P., "Heat Transfer Processes in Rotary Kilns", Ph.D. Thesis, University of British Columbia, Vancouver, B.C. (1986).
- Bayard, R. A., "New Formula Developed for Kiln Time", Chem. Metall. Eng. 100-102, (1945) March.
- Brebba, C. A., J. C. F. Telles and L. C. Wrobel, "Boundary Element Techniques: Theory and Applications in Engineering", Springer-Verlag, Berlin (1984).
- Carley-Macaulay, K. W. and M. B. Donald, "The Mixing of Solids in Tumbling Mixers — I.", Chem. Eng. Sci. 17, 493-506 (1962).
- Carley-Macaulay, K. W. and M. B. Donald, "The Mixing of Solids in Tumbling Mixers — II.", Chem. Eng. Sci. 19, 191-199 (1964).
- De Vahl Davis, G. and G. D. Mallinson, "False Diffusion in Numerical Fluid Mechanics", Univ. of New South Wales, School of Mech. and Ind. Eng. Rept. 1972/FMT/1 (1972).
- Friedman, E. and A. Marshall, "Studies in Rotary Drying", Chem. Eng. Prog., 45, 482 (1949).
- Heiligenstaedt, W., "Thermique appliquée aux fours industriels — Tome II", Paris: Dunod (1971).
- Henein, H., J. K. Brimacombe and A. P. Watkinson, "Experimental Study of Transverse Bed Motion in Rotary Kilns", Metall. Trans. B, 14B, 191-205 (June 1983).
- Henein, H., J. K. Brimacombe and A. P. Watkinson, "The Modeling of Transverse Solids Motion in Rotary Kilns", Metall. Trans. B, 14B, 207-220 (June 1983).
- Kramers, H. and P. Croockewit, "The Passage of Granular Solids Through Inclined Rotary Kilns", Chem. Eng. Sci. 1, 259-265 (1952).
- Kunii, D. and O. Levenspiel, "Fluidization Engineering", John Wiley & Sons, New York (1962), pp. 370-371.
- Lehmberg, J. M. Hehl and K. Schugel, "Transverse Mixing and Heat Transfer in Horizontal Rotary Drum Reactors", Proc. Intern Conf SPIRE, Arad, Israel, December (1975).

- Maeda, T. and F. Matsunaga, "A Survey Note on non-Newtonian Fluid Flow Simulation", Phoenix Users Conference, Dubrovnik, Yugoslavia, 28 August — 2 September (1989).
- Miller, R. W., "Flow Measurement Engineering Handbook", McGraw-Hill, New York (1983), pp. 5-10 - 5-15.
- Mu, J. and D. D. Perlmutter, "The Mixing of Granular Solids in a Rotary Cylinder", AIChE J. 26, 928-934 (1980).
- Patankar, S. V., "Numerical Heat Transfer and Fluid Flow", McGraw-Hill, Toronto (1980).
- Perron, J. and R. T. Bui, "Rotary Cylinders: Solid Transport Prediction by Dimensional and Rheological Analysis", Can. J. Chem. Eng. 68, 61-68 (1990).
- Perry, R. H., C. G. Chilton and S. D. Kirkpatrick, (Ed.), Chemical Engineers' Handbook, McGraw-Hill, New York (1961).
- Ronco, J. J., "Tecnologia de las Operaciones y Los Procesos de la Industria y Quimica 20, 605-614 (1960).
- Rutgers, R., "Longitudinal Mixing of Granular Material Flowing through a Rotating Cylinder. Part I Descriptive and Theoretical", Chem. Eng. Sci. 20, 1079-1087 (1965).
- Ryhming, I. L., "Dynamique des fluides" Presses Polytechniques Romandes, Lausanne (1985) pp. 193-200.
- Saeman, W. C., "Passage of Solids through Rotary Kilns: Factors Affecting Time of Passage", Chem. Eng. Prog. 47, 508-514 (1951).
- Schugel, K., "Rheological Behavior of Fluidized Systems", in Fluidization, J. F. Richardson and D. Harrison (Ed.), Academic Press, London (1971), pp. 261-292.
- Sha, W. T. and S. L. Soo, "Numerical Modeling of Fluidized Bed Combustor", Tech. Memo, ANL-CT-78-4, Argonne National Laboratory, Chicago, IL, November (1977).
- Sullivan, J. D., C. G. Maier and O. C. Ralston, U.S. Bureau of Mines Technical Papers (1927), p. 384.
- Tscheng, H. S., "Convective Heat Transfer in a Rotary Kiln", Ph.D. Thesis, University of British Columbia, Vancouver, B.C. (1978).
- Vahl, L. and W. G. Kingma, "Transport of Solids through Horizontal Cylinders", Chem. Eng. Sci. 1, 253-258 (1952).
- Zablony, W. W., "The Movement of the Charge in Rotary Kilns", Int. Chem. Eng. 5, 360-366 (1964).
- Zienkiewicz, O. C., "The Finite Element Method", 3rd ed., McGraw-Hill, Maidenhead, U.K. (1977).

Manuscript received January 2, 1990; revised manuscript received September 25, 1990; accepted for publication February 10, 1991.